Radiofrequency forward Mössbauer scattering method in study of magnetic materials

**E. K. Sadykov · G. I. Petrov · V. V. Arinin ·
F. G. Vagizov · E. V. Voronina**

Abstract Mössbauer spectra in forward scattering scheme were measured for iron borate ($FeBO_3$) exposed to radiofrequency (rf) field below the Neel temperature. The spectra have satellites spaced by doubled rf field frequency. The semiclassical model of Mössbauer transmission through a thick magnetic sample under rf reversals of a hyperfine field is proposed. This model reproduces all features of the measured spectra. Experiments and model calculations indicate additional possibilities of this measurement scheme for study the soft magnetic materials.

Keywords Mössbauer forward scattering · Quantum interference · Radiofrequency thickness effects · Magnetic materials

1 Introduction

Forward scattering (fs) Mössbauer spectra of thick stainless steel sample excited by coherent ultrasound (us) field were measured first time by authors of [1, 2]. Satellite structure of fs spectra was demonstrated in these experiments. Later the semiclassical theory of Mössbauer
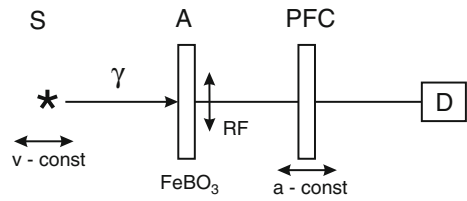
E. K. Sadykov · V. V. Arinin (✉) · F. G. Vagizov · E. V. Voronina
Kazan Federal University, 18 Kremlyovskaya, Kazan 420008, Russia
e-mail: varininse@mail.ru

E. K. Sadykov
e-mail: esad@ksu.ru

G. I. Petrov
Kazan State Power-Engineering University, 51 Krasnoselskaya, Kazan, Russia

                                              Springer

Fig. 1 The scheme of the experimental set-up for measuring forward scattering Mössbauer spectra

radiation transmission through an absorber under the ultrasound field action was proposed [3]. The main goal of this investigation was to reveal the conditions when the radiation intensity increase at the absorber output can be achieved. In this report we present the results of similar fs experiments on iron borate ($FeBO_3$), subjected to influence of rf magnetic field, oscillating in a sample plane. Now we deal with the sample having a magnetic hyperfine structure. There are also several possible mechanisms of rf influence on Mössbauer spectra forming process in this case. These features stimulate the detailed analysis of rf effects in the forward scattering spectra with the purpose of increasing the efficiency of Mössbauer methods for applications in magnetic materials studies.

2 The experimental scheme

The scheme of fs experiment is presented on Fig. 1. Note first of all, acquisition of fs spectra is carried out at constant velocity of the Mössbauer source **S** relative to an absorber **A**. Now the spectrum of Mössbauer radiation transmitted through an absorber (target) is analyzed by second absorber moving with constant acceleration. The $FeBO_3$ single crystal platelet (with thickness 45 μm and planar sizes of order of 4 mm) was used as a sample under investigation. It was cut along the easy magnetization plane (111) of $FeBO_3$ single crystal. One was enriched up to 95 % by isotope ^{57}Fe. The sample was placed inside of the rf coil, which produced the radiofrequency magnetic field, oscillating in the plane of the absorber. The HF-generator, working at the frequency range of 10–30 MHz, provided the maximum amplitude of the rf magnetic field H_{rf} on the sample up to 15 Oe. The sample temperature was kept below the Neel temperature by means of thermostat. The potassium hexacyanoferrate (II) trihydrate, known also as potassium ferrocyanide (**PFC**), with a single absorption line was used as analyzer. The radiation was detected by the detector **D** with thin NaI(Tl) scintillator.

The structure of fs spectra (emission spectra behind an absorber) of magnetic material subjected to rf field is very similar to the structure of fs spectra in acoustical experiments [1–3]. Nevertheless, there is a difference between them. The fs spectra of magnetic materials essentially depend on the experimental conditions. At room temperature the satellites are weak, and they are separated from each other by the rf field frequency, Ω. When the sample temperature approaches to the magnetic transition point ($T_N = 348 K$) the satellites become more intensive and the distance between them equals to 2Ω. On Fig. 2 the fs spectra of $FeBO_3$ measured at $T = 343 K$ for various frequencies of rf field are presented. If the experiments are made under constant magnetic field aligned along the absorber plane in direction perpendicular to linearly oscillating rf field and the value of constant field exceeds the rf field amplitude, then the distance between satellites becomes again equal to Ω (Fig. 3).

The observed dynamics of the fs spectra indicates that at room temperature we deal with rf magnetostriction effect, and near to the magnetic transition point we, more likely, have

Fig. 2 Mössbauer fs spectra of $FeBO_3$ under rf reversals of hyperfine field at temperature $T = 343K$ (**a**, **b**, **c**, **d**, **e**) and $T = 333K$ (**c'**): (**a**) $\Omega = 6, 2MHz$; (**b**) $\Omega = 8MHz$; (**c**) $\Omega = 12MHz$; (**c'**) $\Omega = 12MHz$; (**d**) $\Omega = 15MHz$; (**e**) $\Omega = 19MHz$. $H_{rf} = 4Oe$ and Mössbauer thickness $t_e = 135$ (result of fitting)
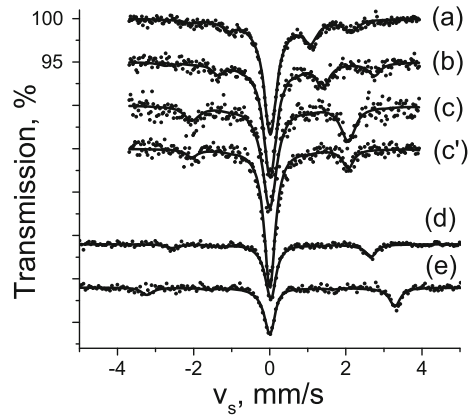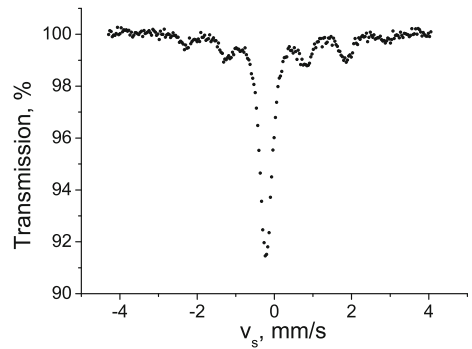
Fig. 3 The fs spectrum of $FeBO_3$ in constant magnetic field ($H_0 = 17Oe$) aligned along the absorber plane in the direction normal to linearly oscillating rf field ($H_{rf} = 4Oe$, $\Omega = 12MHz$); distance between satellites equal to $n\Omega$, $n = 1, 2, 3$

the effect of rf reversals of a hyperfine field. This assumption is supported by small values of planar magnetic anisotropy of $FeBO_3$ crystal and by relatively high temperature used in experiment ($T \lesssim T_N$). Indeed, the model based on hyperfine field reversals reproduces experimental spectra with even satellites [4]. Besides, it adequately describes the fast decrease of the satellite intensities in our experiment with increasing the order number (contrary to the behavior of acoustical satellites [1–3]).

3 The RF hyperfine field reversals model

The transmission of monochromatic gamma wave $E_\omega(y, t) \exp(i(ky - \omega t))$ through the absorber experiencing the rf hyperfine field reversals has been described in [4]. The basic supposition of this model is an appearing of periodical time dependence in the amplitude factor $E_\omega(y, t)$ under rf field action, so it can be presented as $E_\omega(y, t) = \sum_l E_l(y) \exp(-i\Omega lt)$, where $\Omega = 2\pi/T$ – frequency of rf field. Further we use the amplitudes of harmonics $E_l^s(y)$ on depth y in absorber, taking into account the polarization state of gamma radiation s also. These amplitudes satisfy to the set of equations [4]:

$$\partial E_l^s \big/ \partial y = \sum_l G_{ll'}^{ss'} E_{l'}^{s'}(y), \tag{1}$$

$$G_{ll'}^{ss'} = i\sigma_0 N_0 f_{L-M} \Gamma \sum_{q,mM} \frac{A_{mM}^{ss'} a_{q-l}^{mM*} a_{q-l'}^{mM} \exp{(i\varphi(l-l'))}}{4(\omega_a - \omega - \Omega q - i\Gamma/2)}. \tag{2}$$

For solving the set of (1) the boundary conditions $E_l^s(0) = \theta_\omega \cdot \delta_{0l} \cdot \delta_{ss_0}$ must be taken into account, where θ_ω is the Fourier transformation of source radiation, usually having the Lorentz type form, $\theta_\omega = (\Gamma_s/2\pi)^{1/2}(\omega_s - \omega + i\Gamma_s/2)^{-1}$, and s_0 is its polarization index.

The matrix $G_{ll'}^{ss'}$ is responsible for Raman scattering processes of gamma quanta in an absorber with a possible change $l \to l'$ of harmonica's frequency and their polarization $s \to s'$; σ_0 and f_{L-M} – the maximum cross-section of nuclear resonance absorption and Lamb-Mössbauer factor, N_0 – concentration of Mössbauer nuclei, φ – phase of rf field. Expression (2) is received for stepwise rf reversals of hyperfine field B_{hf}. Besides, the coherent hyperfine field reversals on nuclei within the entire volume of the absorber are supposed [3, 4]. Note, the matrix $G_{ll'}^{ss'}$ includes contributions of all possible transitions mM between Mössbauer sublevels m and M of ground and excited nuclear states. In (2) the Fourier coefficients a_n^{mM} for the exponent of periodical function $S(t)$ are introduced: $\exp{(i\Omega_{mM}S(t))} = \sum_n a_n^{mM} \exp{(-in(\Omega t + \varphi))}$. The function $S(t)$ relates to stepwise function $\Phi(t)$ describing the periodical hyperfine field reversals as $S(t) = \int_0^t \Phi(\tau)d\tau$ [4, 5]. The Fourier coefficients a_n^{mM} are given by expression [4]:

$$\begin{aligned} a_n^{mM} &= \frac{2i\Omega_{mM}(1-\exp(-i\Omega_{mM}T/2)(-1)^n)}{T[(\Omega n)^2 - \Omega_{mM}^2]}, \\ \Omega_{mM} &= (\gamma_g m - \gamma_e M)B_{hf} = (\varepsilon_g m - \varepsilon_e M). \end{aligned} \tag{3}$$

In our experiments the quantization axis lays in the plane of the sample. For Mössbauer radiation transmitting through the absorber perpendicularly to the sample plane, the forward scattering takes place on hyperfine transitions mM, having definite linear polarizations, s. In this case $A_{mM}^{ss'} = \delta_{ss'} A_{mM}^s$, where the parameter A_{mM}^s determines the normalized relative intensity of gamma transition mM [4, 5].

Modelling of fs spectra on the basis of equations system (1) includes the calculation of coefficients $G_{ll'}^{ss'}(\omega_a, \omega, \varphi = 0)$ of matrix $\bar{\bar{G}}$ and the numerical solution of this system. The order of system is chosen so to ensure convergence of the solution. The gamma wave on depth y of the absorber, initiated by the Fourier component (with frequency ω and amplitude θ_ω) of source radiation on absorber input, is equal:

$$E_\omega(y, t, \varphi) = \sum_l E_l(y, \varphi) \exp{(-i(l\Omega t + \omega t))}, \tag{4}$$

where $E_l(y, \varphi)$ are a solution of the set of (1):

$$E_l(y, \varphi) \sim \theta_\omega \left\{ \exp\left(\bar{\bar{G}}(\omega_a, \omega, \varphi = 0)y\right) \right\}_{l0} \cdot \exp{(il\varphi)}. \tag{5}$$

The Fourier transformation of (4) is:

$$E_\omega(y, \tilde{\omega}, \varphi) = \sum_l E_l(y, \varphi)\delta(\tilde{\omega} - l\Omega - \omega). \tag{4'}$$

Now we define the intensity of source radiation after its forward scattering by target. Firstly we define the intensity corresponding to field (4'). This result must be integrated on ω and averaged on phases in the interval $0 \le \varphi \le 2\pi$ taking into consideration the expression

$\theta_\omega = \left(\Gamma_s/2\pi\right)^{1/2} \left(\omega_s - \omega + i\,\Gamma_s/2\right)^{-1}$ for Lorentz type form of source radiation. The final fs spectrum expression is:

$$I(\tilde{\omega}, y, \omega_s, \omega_a) = \left(\int |E_\omega(y, \tilde{\omega}, \varphi)|^2 d\omega\right)_\varphi$$

$$= \Gamma_s/2\pi \sum_l \frac{\left|\left\{\exp\left(\bar{\bar{G}}(\omega_a, \tilde{\omega} - l\Omega, \varphi = 0)y\right)\right\}_{l0}\right|^2}{(\omega_s - \tilde{\omega} + l\Omega)^2 + (\Gamma_s/2)^2}. \tag{6}$$

This spectrum is convoluted with an analyzer line form function $\varphi_A(\tilde{\omega}, \tilde{\omega}_A) = t_{an}\left(\Gamma_{an}/2\right)^2 \left[(\tilde{\omega} - \tilde{\omega}_A)^2 + \left(\Gamma_{an}/2\right)^2\right]^{-1}$, resulting in the *model spectrum* used as a key expression in *experimental spectra fitting* (see solid line curves in Fig. 2):

$$I_{an}(\tilde{\omega}_A, y, \omega_s, \omega_a) \sim \int d\tilde{\omega} I(\tilde{\omega}, y, \omega_s, \omega_a) \exp(-\varphi_A(\tilde{\omega}, \tilde{\omega}_A)). \tag{7}$$

$t_{an}, \Gamma_{an}, \tilde{\omega}_A$ – effective thickness, line width and resonance frequency for the analyzer.

Integrating the expression (6) on $\tilde{\omega}$ we obtain the transmission integral as a function of ω_s:

$$T(\omega_s, \omega_a, y) \sim \int d\tilde{\omega} I(\tilde{\omega}, y, \omega_s, \omega_a). \tag{8}$$

Thus the model under discussion may be also used in analyzing the effects of thickness in absorption spectra of Mössbauer samples under rf field. It means, we can expect some qualitative changes in absorption Mössbauer spectra parameters in these conditions.

4 The model calculations

As we have noted above, the fs Mössbauer spectra of magnetic system due to rf hyperfine field reversals in many respects are similar to the spectra of stainless steel foils in the ultrasound field [1–3]. This similarity of the spectra for two systems of different nature was noted in [6] and its physics has been discussed in [4]. At the same time, the formation of fs spectra for magnetic materials are of special interest because it needs to be more understandable for use of the expected rf effects in practice. First of all, now we are interested in the role of hyperfine interaction and rf collapse phenomenon, i.e. peculiar factors for Mössbauer spectra of magnetic systems, in the spectra formation. The another question is closely related with the optimal experimental parameters (optimal velocity of the source, effective thickness of the sample, optimal frequency of rf field) which are necessary to observe the satellite structure of the fs spectra. And at last, the rf mechanisms which cause any change of radiation intensity at the absorber output are of interest also. The answer to these questions can be received on the basis of model calculations in the framework of a model used above. The modelling calculations indicate on possibility to get the additional experimental information using the fs Mössbauer scheme. Below the Mössbauer response of the isotope ^{57}Fe in magnetic sample in conditions of rf hyperfine field reversals taking into account only one nuclear gamma transition $m \rightarrow M$ (further denoted as mM) is calculated. Transmission of gamma radiation through such hypothetical absorber, as we shall see, in many respects is similar to its propagation in single line absorber excited by sound. Besides we point out three types of processes induced in an absorber by rf field (4.1, 4.2, 4.3 indicated further as $i = 1, 2, 3$).

4.1 Gamma radiation interacts with nuclei due to mM transition only, rf field is absent

In this trivial case the spectrum of source radiation after its forward scattering on the sample with effective thickness $t_e = \sigma_0 N_0 f_{LM} y$ can be derived consistently applying expressions (1)–(6) from Section 3 (for example, compare with [7]):

$$I_1^{mM}(\omega, \omega_s, \omega_a, t_e) = \frac{\Gamma_s}{2\pi} \frac{1}{(\omega - \omega_s)^2 + (\Gamma_s/2)^2}$$
$$\times \exp\left[\frac{-t_e A_{mM} \Gamma^2/4}{(\omega_a - \omega + \Omega_{mM})^2 + (\Gamma/2)^2}\right]. \tag{9}$$

At values $\omega_s \simeq \omega_a + \Omega_{mM}$ this formulae describes the fs process, where ω_s, Γ_s (ω_a, Γ_a) are source (absorber) line parameters and Ω_{mM} is defined by hyperfine interaction.

4.2 Gamma radiation interacts with nuclei due to mM transition only, rf field causes the in-phase field reversals on nuclei

Let us define the fs spectrum according the algorithm outlined in Section 3. The slowly varying amplitude $E_{\omega'}(y, t)$ of source radiation is represented by Fourier series:

$$E_{\omega'}(y, t) = E_{\omega'0}(y, t) \exp(-i\omega' t),$$
$$E_{\omega'0}(y, t) = \sum_k E_k(y, \omega') \exp(-ik\Omega t). \tag{10}$$

Now, only one term (mM) in expression (2) must be used as the matrix of coefficients $G_{ll'}^{ss'}$ in the set of equations (1) for unknown parameters $E_k(y, \omega')$. According to theorem for Fourier coefficients $\sum_n a_{n+q}^{mM*} a_n^{mM} = \delta_{q0}$ the system (1) having infinite order can be solved by an iterative method. Instead of (4) the following analytical solution can be received:

$$E_k(y, \omega') = \theta_{\omega'} \exp(-ik\varphi) \sum_q a_{k+q}^{mM*} a_q^{mM} \exp\left(\frac{ik_\gamma y}{2} G_q(\omega')\right), \tag{11}$$

where $G_q(\omega') = \sigma_0 N_0 f_{LM} A_{mM} \Gamma / 2k_\gamma \left(\omega_a - \omega' + q\Omega - i\Gamma/2\right)$ and φ – phase of rf field.

The Fourier transformation of the resulting gamma wave, as follows from (10), looks as:

$$E_{\omega'}(y, \omega, \varphi) = \sum_k E_k(y, \omega') \delta(\omega - k\Omega - \omega').$$

The total contribution to the fs spectrum, taking into account $\theta_{\omega'} = (\Gamma_s/2\pi)^{1/2}(\omega_s - \omega' + i\Gamma_s/2)^{-1}$ for the Lorentz type radiation of source, is defined by expression $I_2^{mM}(\omega, y, \omega_s) = \left(\int |E_{\omega'}(y, \omega, \varphi)|^2 d\omega'\right)_\varphi$, which can be finally represented as:

$$I_2^{mM}(\omega, \omega_s, \omega_a, t_e) = \frac{\Gamma_s}{2\pi} \times \sum_k \frac{\left|\sum_q a_{q+k}^{mM*} a_q^{mM} \exp\left\{\frac{it_e A_{mM} \Gamma/4}{\omega_a - \omega + \Omega(q+k) - i\Gamma/2}\right\}\right|^2}{(\omega_s - \omega + k\Omega)^2 + (\Gamma_s/2)^2}. \tag{12}$$

This formula is an analogue of the expression for the fs spectrum in an acoustic field [3]. Unlike (9) it has satellite structure. The satellites in (12) are separated from each other (see Fig. 4a) on $n\Omega$, $n = 1, 2, 3...$ and they are a result of coherent forward Raman scattering of gamma radiation in the conditions of in-phase hyperfine field reversals [4, 5]. Unlike the usual Mössbauer absorption and emission spectra, the intensity of the fs spectrum satellites induced by periodic perturbation is comparable to intensity of a base line only in the case
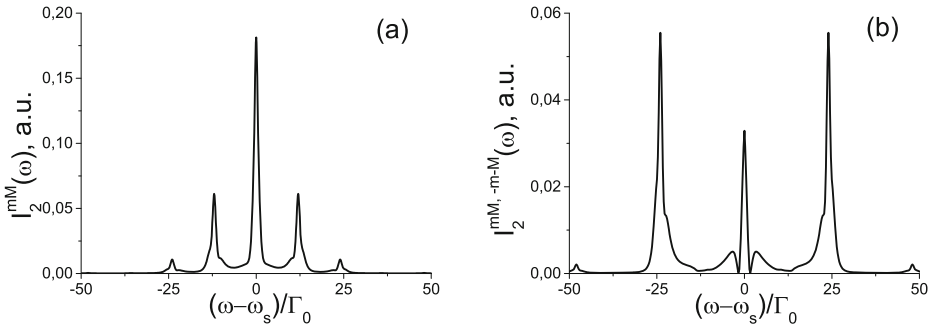
Fig. 4 The fs spectrum for linear polarized ($s = 1$) Mössbauer source radiation calculated taking into account: (**a**) one hyperfine transition $mM = 1/2 \to 1/2$, (**b**) two transitions ($mM = 1/2 \to 1/2; -1/2 \to -1/2$) related by chiral symmetry. The linear polarization $s = 1$ coincides with the polarization of $mM = 1/2 \to 1/2$ transition. $\Omega = 12\Gamma_0$, $\varepsilon_e/\hbar = -10\Gamma_0$, Γ_0 – the natural linewidth, $\omega_s - \omega_a = 0$, $t_e = 100$

of relatively thick absorbers. So, the formation of satellites in the fs spectra for absorbers subjected to periodic fields, and also the increase of a radiation intensity at the absorber output related to this process (see more low) must be classified as the *effects of a sample thickness*.

4.3 The gamma radiation interacts with nuclei due to mM transition only, rf field reversals on nuclei are chaotic in phase

In the case of stochastic hyperfine field reversals we come to other matrix of coefficients, instead of (2). Now we deal with a matrix $G_{ll'}^{ss'}$ diagonal on indices, l, l'. The fs spectrum in this case is:

$$
I_3^{mM}(\omega, \omega_s, \omega_a, t_e) = \frac{\Gamma_s}{2\pi} \frac{1}{(\omega_s - \omega)^2 + (\Gamma_s/2)^2}
$$

$$
\times \prod_q \exp\left\{ \frac{-\left|a_q^{mM}\right|^2 t_e A_{mM}\Gamma^2/4}{(\omega - \omega_a - q\Omega)^2 + (\Gamma^2/4)} \right\}. \tag{13}
$$

For $\omega_s \approx \omega_a + q\Omega$ this expression presents the fs spectrum, which does not contain now satellites because the Raman scattering amplitudes interfere destructively. The expressions (9), (12), (13) are immediately applicable to experimental spectra, if the source radiation polarization coincides with characteristic polarization s of a transition mM. For our geometry of experiment: $A_{mM} \equiv A_{mM}^s$ (see [4, 5]).

The integration of expressions (9), (12), (13) for fs spectra $I_i^{mM}(\omega, \omega_s, \omega_a, t_e)$ ($i = 1, 2, 3$ identify the rf excitation conditions) on frequency ω yields *a transmission integrals*, $T_i^{mM}(\omega_s, t_e)$. Obviously, the integral $T_i^{mM}(\omega_s, t_e)$ is a total intensity of the radiation transmitted through an absorber, which consists of the intensity of base line $T_{i0}^{mM}(\omega_s, t_e)$ and the intensity of its satellites, $T_{i\_sat}^{mM}(\omega_s, t_e)$:

$$
T_i^{mM}(\omega_s, t_e) = T_{i0}^{mM}(\omega_s, t_e) + T_{i\_sat}^{mM}(\omega_s, t_e). \tag{14}
$$

For this hypothetical case (i.e. for the single mM gamma transition) the Mössbauer *absorption spectrum* related to transmission integral can be defined by expression $\varepsilon_i^{mM}(\omega_s, t_e) =$
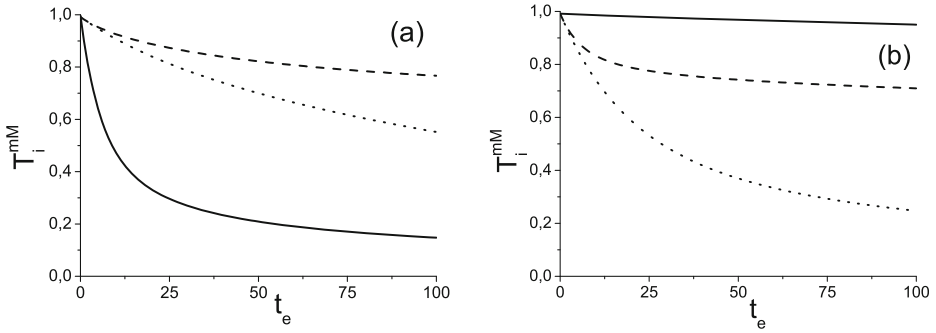
Fig. 5 Transmission integral dependence (for isotope ^{57}Fe) on effective absorber thickness for linear polarized source radiation ($s = 1$): $\varepsilon_e/\hbar = -10\Gamma_0$, $\Omega = 12\Gamma_0$, the single transition $mM = 1/2 \to 1/2$ is taken into account only. *Solid line* – rf field is absent ($i = 1$), *dashed line* – the field reversals are in phase ($i = 2$), *dotted line* – field reversals are not correlated ($i = 3$). (**a**) Source radiation frequency is tuned to single transition ($\omega_s = \omega_a + \Omega_{1/2\to1/2}$), (**b**) source radiation frequency is out of resonance ($\omega_s = \omega_a$)

$f_s \left\{ 1 - T_i^{mM}(\omega_s, t_e) \right\}$, which contains an information about the sample thickness effects. Another parameter, dependent on thickness, is the *integral absorption*, $S_i^{mM}(t_e) = \int \varepsilon_i^{mM}(\omega_s, t_e)d\omega_s$.

The analysis of the dependencies of transmission integrals $\left(T_i^{mM}(\omega_s, t_e)\right)$ versus the effective thickness of absorber $t_e = \sigma_0 N_0 f_{LM} y$ allows us to point out *two* mechanisms of the sample transparency change due to rf hyperfine field reversals. *First* of them is related to the appearance of rf collapse phenomenon. The transparency can be increased or decreased depending on the resonance condition at rf field absence. For example, if $\omega_s = \omega_a + \Omega_{1/2\to1/2}$ (i.e. the source line is tuned to the frequency of transition, $\left|I_g, m = 1/2\right\rangle \to \left|I_e, M = 1/2\right\rangle$) the rf field reversals destroy a resonance condition and lead to increase of the transmission integral, $T_2^{mM} > T_3^{mM} > T_1^{mM}$, for all effective thickness values (see the Fig. 5). On the contrary, if the source line does not resonate with transition mM in absence of rf field, the switching on the rf field leads to partial restoration of a resonance condition (Fig. 5b), so we have a relationship: $T_1^{mM} > T_2^{mM} > T_3^{mM}$.

The inequality $T_2^{mM} > T_3^{mM}$ in both cases considered above (resonant and nonresonant) is a consequence *of second* mechanism of the rf transparency. One is a result of coherent Raman scattering of gamma quanta in forward direction in case $i = 2$. This type of the radiation yield enhancement in fs Mössbauer experiments was investigated first time in stainless steel under coherent sound action [3], where the forming of superpositional states of gamma radiation field in an absorber was shown. In close analogy to [3], for our (rf) case the envelope of gamma wave (10) can be rewritten as a linear combination of superpositional states, $\Sigma_q(\Omega, t)$:

$$E_{\omega0}(y, t) = \sum_k E_k(y, \omega') \exp(-ik\Omega t) = \theta_{\omega'} \sum_q a_q^{mM} \Sigma_q(\Omega, t) \exp\left(\frac{ik_\gamma y}{2} G_q(\omega')\right),$$
(15)

where $\Sigma_q(\Omega, t) = \sum_k a_{k+q}^{mM*} exp(-(\Omega t + \varphi)k) = \exp(i(\Omega t + \varphi)q - \Omega_{mM} S(t))$.

The important property of superpositional states $\Sigma_q(\Omega, t)$ is the independence of their spectral distribution versus absorber thickness. At a given frequency ω' one of states, for example $\Sigma_0(\Omega, t)$, has an considerable absorption, while others $\Sigma_q(\Omega, t)$ with $q \neq 0$ have anomalous small absorption coefficients. In absence of in-phase rf reversals there are no superpositional states. Hence, now there are no states with anomalous small absorption.

Fig. 6 The dependence of $S_i^{mM}(t_e)$ on effective thickness for model absorber ($mM = 1/2 \rightarrow 1/2$ transition only). The source radiation of linear polarization $s = 1$ is supposed; $\Omega = 12\Gamma_0$, $\varepsilon_e/\hbar = -10\Gamma_0$. *Solid line* – rf field is absent ($i = 1$), *dashed line* – the field reversals are in phase ($i = 2$), *dotted line* – field reversals are not correlated ($i = 3$).
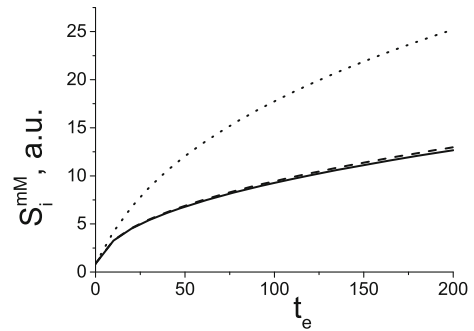
Further, let us compare the dependencies of integral absorption parameters S_i^{mM} as the functions of an effective absorber thickness for cases discussed above, $i = 1, 2, 3$ (Fig. 6). The inequality $S_2^{mM} < S_3^{mM}$ is expected in view of the enhancement of transmission integral due to coherent Raman scattering of gamma quanta. The increasing of integral absorption S_3^{mM} relative to S_1^{mM} is also explainable by a change of the saturation effect [8, 10] due to appearing of sideband structure of absorption spectrum in case $i = 3$. Recently the similar phenomenon was observed experimentally [11] in absorption spectra of $FeBO_3$ as a result of the rf excitation. The increase of integral absorption parameter for the sample under rf field was found there and interpreted as the rf suppression of the resonant absorption saturation in thick absorbers. Modelling of experiment [11] was made in the assumption of magnetostriction oscillations in the sample and of Rayleigh distribution for their amplitudes. The integral absorption used for description of the experiment [11] was of S_3^{mM} type, when the mechanism of forming of superpositional states is excluded. Now we return to the result of our calculations, $S_1^{mM} < S_3^{mM}$ (Fig. 6), and consider it as an analogue of effect in [11], – i.e. as *the suppression of thickness saturation effect in the conditions of random rf field reversals* on nuclei of the absorber. On the contrary, the result $S_2^{mM} \approx S_1^{mM}$ means that *no effect of such suppression is available in case of phase correlated field reversals*.

The result of calculations, $S_2^{mM} \approx S_1^{mM}$, presented on Fig. 6, is valid for a wide range of effective thickness and values of rf frequencies. It means, that the integral absorption attains a minimum, contrary to relationship $S_1^{mM} < S_3^{mM}$, if the periodic field reversals on nuclei are in phase. This minimum is limited by value of integral absorption in case of absence of reversals. Thereby we come to relationships for estimation of the forward Raman scattering contribution to rf gamma transparence.

The modelling of fs spectra *for real magnetic systems* turns us to necessity to use a summation over mM in (2). It means, that the formation of fs Mössbauer spectra in real magnetic systems has to include the *quantum interference* (QI) [12, 13] of fs amplitudes for all transitions mM. In this case the rf effects to be displayed in Mössbauer spectra must be given by parameters $I_i^{\Sigma}(\omega, \omega_s, \omega_a, t_e)$, $T_i^{\Sigma}(\omega_s, t_e)$, $S_i^{\Sigma}(t_e)$, instead of $I_i^{mM}(\omega, \omega_s, \omega_a, t_e)$, $T_i^{mM}(\omega_s, t_e)$, $S_i^{mM}(t_e)$, for three regimes of rf perturbation of the system ($i = 1, 2, 3$). In general case the calculation of $I_i^{\Sigma}(\omega, \omega_s, \omega_a, t_e)$ is made by a numerical method (see (6)). As a consequence of QI, the odd order satellites of fs spectra of the magnetic samples have to disappear. This was predicted theoretically [14] and was proved in our measurements [4, 5] and model calculations (see Fig. 4).

The model calculations of the parameters $I_i^{\Sigma}(\omega, \omega_s, \omega_a, t_e)$, $T_i^{\Sigma}(\omega_s, t_e)$, $S_i^{\Sigma}(t_e)$, instead of $I_i^{mM}(\omega, \omega_s, \omega_a, t_e)$, $T_i^{mM}(\omega_s, t_e)$ can be used for the preliminary estimation of optimal conditions for the fs Mössbauer experiments to be most successful. For example, in order
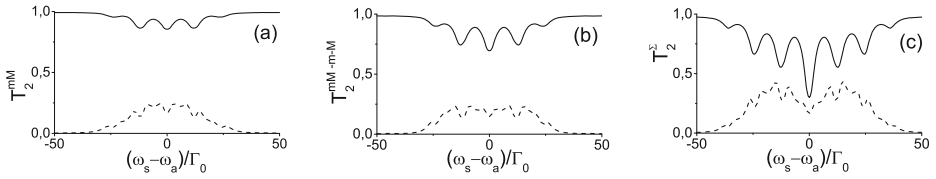
Fig. 7 The transmission integral dependence on frequency ω_s for unpolarized source radiation. $t_e = 100$, $\varepsilon_e/\hbar = -10\Gamma_0$, $\Omega = 12\Gamma_0$. (**a**) $mM = 1/2 \rightarrow 1/2$, (**b**) two hyperfine transitions are taken into account $mM = 1/2 \rightarrow 1/2$; $-1/2 \rightarrow -1/2$, **c** all hyperfine transitions mM are taken into account
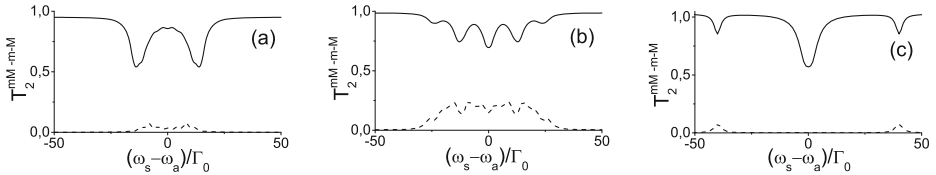

Fig. 8 The dependence of $T_2^{mM,-m-M}(\omega_s)$ (*solid line*) and $T_{2\_sat}^{mM,-m-M}(\omega_s)$ (*dashed line*) on source radiation frequency: $\varepsilon_e/\hbar = -10\Gamma_0$, $\Omega = 12\Gamma_0$, $\omega_s - \omega_a = 0$, unpolarized source radiation is believed and two hyperfine transitions are taken into consideration $mM = 1/2 \rightarrow 1/2$; $-1/2 \rightarrow -1/2$. $t_e = 100$, $\varepsilon_e/\hbar = -10\Gamma_0$, (**a**) $\Omega = 2\Gamma_0$, (**b**) $\Omega = 12\Gamma_0$, (**c**) $\Omega = 40\Gamma_0$

to have the pronounced satellite structure of the fs spectra, the optimal values of ω_s should be estimated using the calculations of the transmission integrals $T_2^{\Sigma}(\omega_s)$ and $T_{2\_sat}^{\Sigma}(\omega_s)$ defined in close analogy to expression (14) (see Fig. 7).

Similar calculations of integrals, $T_2^{mM}(\omega_s)$, $T_{2\_sat}^{mM}(\omega_s)$ and $T_2^{mM,-m-M}(\omega_s)$, $T_{2\_sat}^{mM,-m-M}(\omega_s)$, (Fig. 8) yield information about optimal rf frequencies which allow to get the pronounced satellite structure of the fs spectra, i.e. $\Omega \sim \Omega_{mM}$.

5 Conclusion

1. In this paper the fs Mössbauer spectra of weak ferromagnetic system ($FeBO_3$) subjected to rf field are presented. The results of our study agree in the whole with the experimental data received early [15], i.e. with the rf absorption Mössbauer spectra of iron borate. The appearance of the rf hyperfine field reversals in weak ferromagnetic sample and the collapse of hyperfine structure were studied in these experiments at room temperature and at high radio frequencies (36 and 64 MHz). The magnetostriction sidebands were observed already at very low rf field intensities ($\sim 1.5\ Oe$). At higher field intensities ($\sim 10\ Oe$) the spectra collapsed to the central line accompanied by rf sidebands.

   Our experiments are complementary to the results of [15] in sense of a methodology as well as in experimental conditions. Our Mössbauer measurements were carried out in forward scattering scheme. The sample temperature ($\sim 343\ K$) near the point of magnetic phase transition ($T_N = 348\ K$) has ensured the regime of perfect magnetization reversals even at relatively low rf amplitudes ($2 - 3\ Oe$). On the other hand, at low radiofrequencies the stepwise time dependence model for the alternating hyperfine field is more adequate.

2. The forming of fs spectra under rf hyperfine field reversals in magnetic systems is a result of spatial interference as well as of quantum interference of the Raman scattering amplitudes for gamma quanta. In this case the model for Mössbauer absorption calculation also be modified for thick targets taking into account periodical processes on nuclei under external field. Otherwise, the correct model of absorption has to include possible diffraction phenomena for Raman amplitudes. This requirement is fulfilled naturally if the following scheme of interrelation between forward scattering spectra and the spectra of absorption is used: $I_i^{\Sigma}(\omega, \omega_s) \rightarrow T_i^{\Sigma}(\omega_s) \rightarrow 1 - T_i^{\Sigma}(\omega_s)$.

3. The satellite structure of fs Mössbauer spectra can be an indicator of the phase correlation between field reversals on nuclei. This advantage of fs scheme can be used in order to develop a more effective model for description of rf collapse phenomena in magnetic materials. There is a rich experimental material on absorption Mössbauer spectra [15, 16] displaying rf collapse effect and at the same time having no enough convincing base for their modelling. One of possible reasons for it can be related to absence of more detailed experimental information. Such deficit of experimental details could be compensated in some cases by additional Mössbauer measurements using forward scattering scheme. For example, long time ago Julian and Daniels [17] have offered model of chaotic rf field reversals on the nuclei as the alternative to already available mechanism of rf collapse, i.e. coherent dynamics of magnetization in rf field [18]. Obviously, Julian's model contradicts to the observed satellite structure of fs spectra of iron borate in vicinity of magnetic transition, T_N.

4. The modified experimental method under discussion can be used also to study the magnetic nanostructures, in particular, for investigations of the magnetodynamic properties in radio-frequency fields. Operational properties of these materials in many respects depend on coherence/phase correlation of the processes induced by external perturbation.

References

1. Asher, J., Cranshaw, T.E., O'Connor, L.A.: J. Phys. A Math. Nucl. Gen. **7**, 410 (1974)
2. Tsankov, L.T.: J. Phys. A Math. Gen. **13**, 2969 (1980); ibid, **14**, 275 (1981)
3. Shvyd'ko, Y.V., Smirnov, G.V.: J. Phys. Condens. Matter. **4**, 2663 (1992)
4. Sadykov, E.K., Dzyublik, A.Y., Petrov, G.I., Arinin, V.V., Spivak, V.Y.: JETP Lett. **92**, 250 (2010)
5. Sadykov, E.K., Petrov, G.I., Arinin, V.V., Vagizov, F.G.: Uchenye zapiski Kazanskogo universiteta **154**, 42 (2012)
6. Shvyd'ko, Y.V.: Phys. Rev. B **59**, 9132 (1999)
7. Shpinel, V.S.: Resonans gamma luchei v kristallakh, vol. 407. Moskow, Nauka (1969)
8. Margulies, S., Ehrman, I.: Nucl. Instr. Meth. **12**, 131 (1961)
9. Bykov, G.A., Hien, P.Z.: JETP Lett. **16**, 646 (1963)
10. Williams, J.M., Brooks, J.S.: Nucl. Instr. Meth. **128**, 363 (1975)
11. Vagizov, F.G., Manapov, R.A., Sadykov, E.K., Lyubimov, V.V., Kocharovskaya, O.A.: Hyp. Int. **188**, 143 (2009)
12. Sadykov, E.K., Arinin, V.V., Vagizov, F.G.: JETP Lett. **92**, 431 (2005)
13. Smirnov, G.V., Chumakov, A.I., Potapkin, V.P., Ruffer, R., Popov, S.L.: Phys. Rev. A **84**, 053851 (2011)
14. Dzyublik, A.Y., Spivak, V.Y.: Ukr. J. Phys. **42**, 390 (2002)
15. Kopcevicz, M., Engelmann, H., Stenger, S., Smirnov, G.V., Gonser, U., Wagner, H.-G.: J. Appl. Phys. **44**, 131 (1987)
16. Kopcevicz, M.: J. Alloys Compd. **382**, 165 (2004)
17. Julian, S.R., Daniels, J.M.: Phys. Rev. B **38**, 4394 (1988)
18. Pfeiffer, L., Heiman, N.D., Walker, J.C.: Phys. Rev. B **6**, 74 (1972)